Mathematical Modeling of Hydrogen Production Process by Pressure Swing Adsorption Method

E.I. Akulinin[1]*, A.A. Ishin[2], S.A. Skvortsov[2], D.S. Dvoretsky[1], S.I. Dvoretsky[1]

[1]Department of Technology and Equipment for Food and Chemical Production,
[2] Department of Information Processes and Management, Tambov State Technical University,
1, Leningradskaya St., Tambov, 392000, Russia

* Corresponding author: Tel.: +7(909) 231 40 61; *E-mail*: akulinin-2006@yandex.ru

Abstract

A mathematical model of the dynamics of pressure swing adsorption (**PSA**) process during separating multicomponent gas mixtures to produce hydrogen has been developed. The model includes the equations of mass- and heat transfer processes which occur during adsorption (desorption) of the components (H_2, CO_2 и CO) of gas mixture by granular zeolite adsorbents CaA, NaX, LiLSX; the equation of the kinetics of mixed-diffusive transport of adsorbate (H_2, CO_2 и CO); the Langmuir–Freundlich isotherm equation for multicomponent gas mixtures; the Ergun equation for calculating the pressure and velocity of gas mixture in the adsorber, and allows calculating the profiles of component concentrations (H_2, CO_2 и CO) and temperature in the gas and solid phases, pressure and velocity of the gas mixture along the height of the adsorbent depending on time. As a result of computational experiments, the effect of changes in the temperature, composition, and pressure of the initial gas mixture on the purity, recovery, and production hydrogen temperature at multiple duration periods of the adsorption stage was determined. The dynamics of the adsorption process of gas mixture components and the character of sorption and thermal fronts motion along the height of the adsorbent bed in the adsorber, as well as the relationship between the output of the 4-column PSA unit and the purity of the produced hydrogen have been studied.

Introduction

In recent decades, it has become increasingly common to use cyclic adsorption processes to separate gas mixtures and concentrate target products in them. The adsorption process is the interaction of a bulk phase (gas or liquid) and an adsorbent, during which certain components of the bulk phase are absorbed by the adsorbent; at the output, a concentrated product is obtained, which is the least sorbing component. The adsorption processes with regenerated adsorbent include processes with direct and indirect heat input, and heatless processes. Short-cycle heatless adsorption (called Pressure Swing Adsorption in the English-language literature) represents a special class of adsorption processes. As the name implies, PSA processes do not imply the presence of an external heat source. Due to high rates of adsorption-desorption, compared to heat transfer processes, the heat loss with production gas flow is minimal; thus, the heat released at the adsorption stage is used to desorb the adsorbed components during the regeneration stage of the adsorbent [1–3].

PSA processes are widely used in industry to extract hydrogen from gas mixtures, oxygenate the air, dehydrate gases, separate hydrocarbons, concentrate carbon dioxide, extract methane, and so on. One of the urgent problems in the field of adsorption separation is the production of hydrogen from hydrogen-containing process flows (gases of hydrocarbons conversion and oxidation, refinery gases, synthesis-gas, etc.). Typical substances that accompany hydrogen are nitrogen, carbon oxide and dioxide, methane. The adsorption production of hydrogen is noted for the fact that in

mixtures of hydrogen-containing gases the accompanying components have a higher molecular mass than hydrogen and they are adsorbed more intensively than hydrogen [2].

Hydrogen is widely used in various industries due to its high chemical activity, exceptional lightness and a large amount of heat released during it combustion. It is mainly consumed by oil refining and petrochemical enterprises, where up to 50 % of industrially produced hydrogen is used. In other industries, hydrogen is used both as the main raw material, as an auxiliary material and as fuel. According to statistics, total hydrogen consumption doubles every 15 years.

This work is aimed at: 1) developing a mathematical model of the process of adsorption separation of a gas mixture with a cyclically varying pressure and concentration of hydrogen in it; 2) studying the effect of changes in the temperature, composition and pressure of the initial gas mixture on the purity, recovery and production hydrogen at multiple duration periods of adsorption stage; 3) studying the dynamics of the adsorption process of the gas mixture components and the nature of the sorption and heat fronts motion along the height of the adsorbent bed in the adsorber, as well as the relationship between the output of the 4-column PSA unit and the purity of the hydrogen being produced.

Technology of Adsorption Separation of a Gas Mixture and Hydrogen Production

The technological process of hydrogen concentration by adsorption separation of gas mixture is implemented in a 4-column PSA unit (Fig. 1) [4]. The unit is designed for producing hydrogen with a concentration of 99.99 % vol. from a gas mixture containing hydrogen (65 ± 2) %, carbon dioxide (34 ± 2) % and carbon monoxide (1 ± 0.5) % vol. The initial gas mixture is supplied to the unit after preliminary dehydration (the dehydration stage is not considered in this work) with an excess pressure of 2.1 MPa and a temperature of 30 °C. The pressure rise in the adsorbers $A_1 - A_4$ is provided by opening the controlled
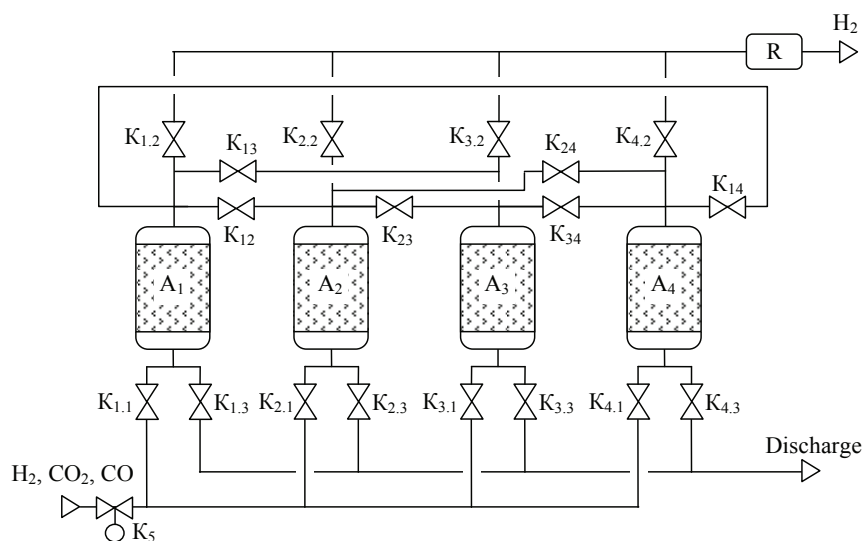

Fig. 1. Process flow diagram of the 4-column PSA unit for hydrogen production:
$A_1 - A_4$ − adsorbers; K − controlled valves; R − receiver

valves $K_{1.1}$, $K_{2.1}$, $K_{3.1}$ and $K_{4.1}$, respectively, through which the gas is supplied to the adsorbent bed. The synthetic zeolite CaA is used as an adsorbent. The production hydrogen is removed from the adsorbers via the controlled valves $K_{1.2}$, $K_{2.2}$, $K_{3.2}$ and $K_{4.2}$ and is directed to the consumers through the receiver P. Countercurrent regeneration of the adsorbent bed in the columns is carried out by passing the purge gas mixture through the valves K_{12}, K_{13}, K_{14}, K_{23}, K_{24} and K_{34}. Through the valves $K_{1.3}$, $K_{2.3}$, $K_{3.3}$ and $K_{4.3}$ the purging gas is discharged at the regeneration stage.

The coordinated operation of the unit valves ensures the sequential passage by each adsorber of all the stages of the cyclic adsorption process, presented in Table 1.

The following designations in Table 1 have been adopted: $A_1 - A_4$ − adsorbers; AD − adsorption; PE − pressure equalizing (gas bypass); GD − gas discharge; R − regeneration; PR − pressure rise.

Granular active carbons and zeolites CaA and NaX, having the largest capacity and selectivity for CO_2 and CO, are widely used as adsorbents in cyclic adsorption processes [1]. At present, the area

Table 1

Stages of the adsorption process of hydrogen production in a 4-column PSA unit

A_1	AD		PE 1	PE 2	GD	R	PE 3	PE 4	PR	
A_2	PE 4	PR		AD		PE 1	PE 2		GD	R	PE 3
A_3	GD	R	PE 3	PE 4	PR		AD		PE 1	PE 2
A_4	PE 1	PE 2		GD	R	PE 3	PE 4	PR		AD

of obtaining composite sorption-active materials (**CSAM**) with prescribed properties is actively developing to be used in cyclic adsorption-desorption processes of hydrogen separation from synthesis-gas [5]. The most promising adsorbents to be used in PSA processes of hydrogen production are CSAM based on liquid and solid amines as well as organometallic compounds (metal hydroxides of Fe, Zr, Co, Ni, Ti). They combine the advantages of zeolites and active coals because they do not adsorb moisture and at the same time can absorb harmful impurities. At present, technology has been developed for obtaining promising adsorbents for absorbing CO_2 and CO when hydrogen is concentrated on the basis of a mesoporous organometallic framework structure in the form of granules with a diameter of 2 mm from hydrated zirconium dioxide stabilized with zinc salts. This type of adsorbent can purify gas mixtures from CO_2 to concentrations of ~5 – 10 ppm.

Mathematical Description of Adsorption Processes with Cyclically Varying Pressure in Gas Mixtures Separation

During adsorption of H_2, CO_2 and CO by a zeolite adsorbent, the following mass- and heat transfer processes proceed: a) diffusion of H_2, CO_2 and CO in a gas mixture flow; b) mass exchange of H_2, CO_2, CO and heat exchange between the gas phase and the adsorbent; c) adsorption of H_2, CO_2, CO on the surface and in micropores of zeolite adsorbent granules with heat release and desorption of H_2, CO_2, CO from micropores and from the surface of granules with heat absorption. Analysis of the results of physical modeling showed that diffusion of H_2, CO_2, CO and heat propagation in the gas flow and granular adsorbent are carried out mainly in the longitudinal direction relative to the flow of the gas mixture in the adsorber (along the height of the adsorbent). The process of hydrogen gas mixture enrichment during adsorption of CO_2 and CO by the granular zeolite adsorbent is carried out in the mixed-diffusion region and is determined by the coefficients of external mass transfer and internal diffusion, as well as equilibrium ratios of the concentrations of H_2, CO_2 and CO in phases.

In the mathematical description of the process of hydrogen enrichment of gas mixture by CO_2 and CO extracting from it in the PSA unit, the following assumptions were made: 1) the initial gas mixture is three-component (it contains 1 – production gas H_2 with a concentration of (65 ± 2) % vol.; 2 – dioxide carbon with a concentration of (34 ± 2) % vol. and 3 – carbon oxide with a concentration of (1 ± 0.5) % vol. and is treated as an ideal gas, which is quite acceptable

at the adsorber pressure of 200 to 10^5 Pa [6]; 2) granulated CaA zeolite with a granule diameter of 1.5 mm, porosity granules coefficient ~0.394 and a diameter of transport pores $d_e \leq 0.5 \times 10^{-3}$ m is used as an adsorbent; 3) the geometric dimensions of the adsorption layer are assumed to be constant for a preset lifetime of ~10^5 h [7]; 4) the adsorbent layer is a continuous medium with a porosity factor ε, which takes into account the porosity of granules; 5) the desorption branch of the sorption isotherms of H_2, CO_2 and CO on the granular CaA zeolite coincides with the adsorption branch [3]; 6) the adsorption equilibrium is described by the Langmuir–Freundlich equation [8].

In accordance with the accepted assumptions, the mathematical description of the process of CO_2, CO extracting from the gas mixture by PSA method and concentrating H_2 in the gas mixture flow includes the following equations.

1. The equation of the componentwise material balance $k = \{1 - H_2, 2 - CO_2, 3 - CO\}$ in the gas mixture flow along the height of the adsorbent bed

$$\frac{\partial c_k(x,t)}{\partial t} + \frac{(1-\varepsilon)}{\varepsilon}\frac{\partial a_k}{\partial t} + \frac{\partial(v_g c_k(x,t))}{\partial x} =$$
$$= \frac{\partial}{\partial x}\left(D_g^k(x)\frac{\partial}{\partial x}c_k(x,t)\right), \qquad (1)$$

where v_g is the gas flow rate (m/s); c_k is molar concentration of the k-th component of the gas mixture (mol/m^3); a_k is the amount of sorption of the k-th component in the adsorbent (mol/m^3); ε is the porosity of the adsorbent taking into account the porosity of granules, (m^3/m^3); D_g^k is effective coefficient of longitudinal mixing of the k-th component in the gas mixture (m^2/s); x is a spatial coordinate of adsorbent bed (height in the adsorber) (m); t is the time (s).

In equation (1), the first term describes the rate of accumulation of the k-th component of the mixture in the gas phase; the second term is the rate of accumulation of the k-th component in the adsorbent; the third term is the convective transfer of substance in the adsorbent bed; the fourth term is the longitudinal mixing of the k-th component in the adsorbent bed.

2. The equation of mass transfer of the adsorbate (H_2, CO_2, CO) from the gas phase to the solid phase of the adsorbent (through the interface):

$$\frac{\partial a_k}{\partial t} = \frac{F_k^2 - F_k^1}{2}tgh\left(\theta\left(v_g - v_g^*\right)+1\right) + F_k^1;$$
$$k = H_2, CO_2, CO, \qquad (2)$$

where F_k^1 is the right-hand side of the equation of the kinetics of non-stationary convective (external) mass transfer, $F_k^1 = \beta_k^1\left(c_k - c_k^*\right)$; β_k^1 is coefficient of mass

transfer, referred to the concentration of adsorbate in the gas phase; c_k^* is equilibrium concentration in a gas phase; F_k^2 is right-hand side of the equation of the kinetics of the intradiffusion adsorption process, $F_k^2 = \beta_k^2(a_k^* - a_k)$; β_k^2 is the kinetic coefficient; a_k^* is adsorption amount or equilibrium concentration in a solid phase; v_g^* is the critical rate of the gas mixture, which determines the transition from the diffusion region (external mass transfer) to the kinetic region (internal diffusion in the adsorbent granules) of the adsorbate transfer (H$_2$, CO$_2$, CO).

Equation (2) is a description of the adsorption kinetics for the mixed-diffusion transport region of adsorbate (H$_2$, CO$_2$, CO) across the interface (Fig. 2): at a gas mixture velocity below v_g^*, the adsorption process is limited by the external mass-transfer process with coefficient β_k^1, otherwise – by the process of internal diffusion in adsorbent granules with kinetic coefficient β_k^2. The hyperbolic tangent and formal coefficient θ allow smoothly adjusting the dimensions of the mixed-diffusion region of the adsorption process CO$_2$ and CO by the adsorbent.

The mass-transfer coefficient β_k^1, formal kinetic coefficients β_k^2 and θ were corrected from experimental data by solving the inverse coefficient problem using the equations of the mathematical model: $v_g^* = 0.022$ м/s; $\beta_{H_2}^1 = 0.816$ s^{-1}; $\beta_{CO_2}^1 = 0.021$ s^{-1}; $\beta_{CO}^1 = 0.084$ s^{-1}; $\beta_{H_2}^2 = 0.73$ s^{-1}; $\beta_{CO_2}^2 = 0.012$ s^{-1}; $\beta_{CO}^2 = 0.059$ s^{-1}; $\theta = 18.2$. The adsorption amount a_k^*, or equilibrium concentration of adsorbate c_k in the flow on the outer surface of the granules, is calculated by the Langmuir–Freindlich formula
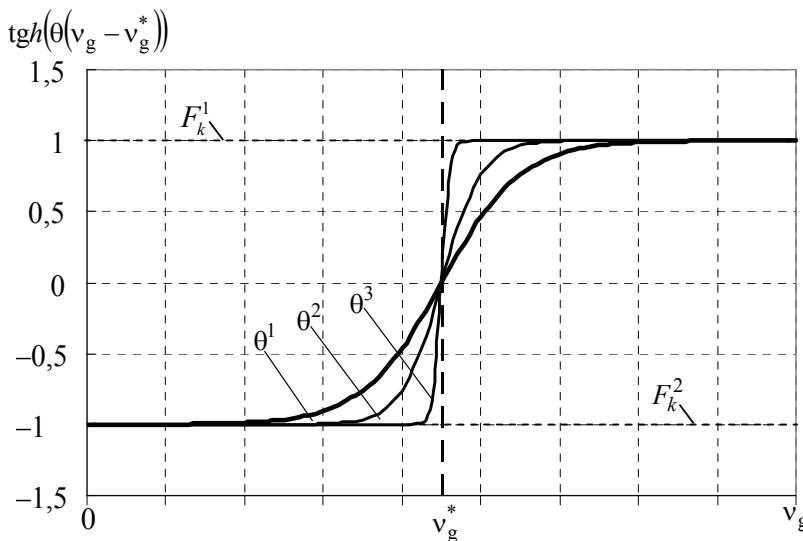

Fig. 2. The effect of θ on the sizes of the mixed-diffusion region

$$a_k^* = \frac{(b_{1,k} - b_{2,k}T_a)b_{3,k}e^{b_{4,k}/T_a}c_k^{(b_{5,k}+b_{6,k}/T_a)}}{1 + \sum_j b_{3,j}e^{b_{4,j}/T_a}c_j^{(b_{5,j}+b_{6,j}/T_a)}},$$

where b is the parameter vector of the sorption isotherm [8]; T_a is the adsorbent temperature.

3. The equation describing the propagation of heat in the gas mixture flow along the height of the adsorbent:

$$c_p^g\rho_g\frac{\partial T_g(x,t)}{\partial t} + c_p^g\rho_g v_g\frac{\partial T_g(x,t)}{\partial x} - \frac{\alpha}{\varepsilon}S_u[T_a(x,t) - T_g(x,t)] =$$
$$= \lambda_g\frac{\partial^2 T_g}{\partial x^2},\ 0 < x < L,\qquad(3)$$

where c_p^g, ρ_g is the specific heat and molar density of the gas mixture, respectively, J/(mol·K), mol/m^3; v_g is velocity of the gas mixture, m/s; T_g is temperature of the gas mixture, K; T_a is the adsorbent temperature, K; λ_g is coefficient of thermal conductivity of the gas mixture, W/(m·K); α is the coefficient of heat transfer from the surface of the adsorbent granules to the gas mixture flow, W/(K·m^2); $S_u = (1-\varepsilon)\dfrac{3}{r_{gr}}$ is the specific surface area coefficient of the adsorbent granules, m^2/m^3; r_{gr} is the radius of the adsorbent granule, m.

In equation (3), the first term describes the accumulation of heat in the gas phase; the second term describes the convective component of heat transfer; the third term – the heat transfer from the gas phase to the solid phase (adsorbent); the fourth term – the longitudinal thermal conductivity of the gas phase along the height of the adsorbent bed.

4. The equation describing the temperature change in the adsorbent

$$c_p^a\rho_a\frac{\partial T_a(x,t)}{\partial t} + \alpha S_u[T_a(x,t) - T_g(x,t)] -$$
$$-\sum_k h_k^a\frac{\partial a_k(x,t)}{\partial t} = \lambda_a\frac{\partial^2 T_a(x,t)}{\partial x^2},\qquad(4)$$

where c_p^a is the specific heat capacity of the adsorbent, J/(kg·K); ρ_a is the adsorbent density, kg/m^3; c_p^g is the specific heat of adsorbate, J/(mol·K); h_k^a is heat of adsorption of the k-th component of the gas mixture, J/mol; λ_a is coefficient of thermal conductivity of the adsorbent, W/(m·K).

In equation (4), the first term describes the enthalpy of the solid phase (adsorbent); the second term describes the heat transfer from the solid phase (adsorbent) to the gas phase; the third term – the heat release of the gas mixture components sorption; the fourth term – the thermal conductivity in the adsorbent along the vertical axis of the adsorber.

5. The Ergun equation describing the change in pressure and velocity of the gas mixture along the height of the adsorbent [9]

$$\frac{\partial P}{\partial x} = -\left(\frac{150(1-\varepsilon_0)^2}{(2r_{gr}\psi)^2\varepsilon_0^2}\mu_g\nu_g + 1.75M_g\rho_g\frac{(1-\varepsilon_0)}{2r_{gr}\psi\varepsilon_0}\nu_g^2\right), \quad (5)$$

where ε_0 is the porosity of the adsorbent bed without taking into account the porosity of the particles, m³/m³; ψ is the sphericity factor of the adsorbent granules; μ_g is the dynamic viscosity of the gas mixture, (H·s)/m²; M_g is Molar mass of the gas mixture, kg/mol.

The initial and boundary conditions for equations (1) – (5) are given in Table 2.

In formulas (7), (8′) S is the cross-sectional area of the adsorber, m².

Formulas for calculating the coefficients of the mathematical model are presented in Table 3.
The effective coefficients of longitudinal mixing of the components of the gas mixture D_g^k were calculated by formulas (9) – (11) [10], where: D_{gm}^k are the molecular diffusion coefficients of the corresponding component, m²/s; D_{12}, D_{13}, D_{23} are molecular diffusion coefficients calculated for a two-component gas mixture, m²/s; M_{g1}, M_{g2}, M_{g3} are molar masses H₂, CO₂, CO, respectively, mol/m³; ϑ_1, ϑ_2, ϑ_3 are diffusion volumes H₂, CO₂, CO, respectively, m³/mol. The initial approximations for the mass-transfer coefficient $\beta_k^{1\,(0)}$ and the formal kinetic

Table 2

The initial and boundary conditions for equations (1) – (5)

Adsorption	Desorption
Initial conditions ($0 \le x \le L$)	
$t = 0: c_k(x,0) = c_k^0(x), \quad a_k(0) = 0, T_g(x,0) = T_g^0(x),$ $T_a(x, 0) = T_a^0(x)$ $k = (1-H_2, 2-CO_2, 3-CO); \quad \nu_g(x,0) = \nu_g^0(x);$ $t = n\tau_{ads}(1+\theta), \quad \theta = \tau_{des}/\tau_{ads}, \quad n = 1,2, ...:$ $c_k^{ads}(x,t) = c_k^{des}(x,\tau_{des}), a_k^{ads}(t) = a_k^{des}(\tau_{des}),$ $T_g^{ads}(t) = T_g^{des}(x,\tau_{des}), \quad T_a^{ads}(t) = T_a^{des}(x,\tau_{des}),$ $\nu_g^{ads}(x,t) = \nu_g^{des}(x,\tau_{des})$ (6)	$t = (n+n\theta-\theta)\tau_{ads}, n=1,2,...:$ $c_k^{des}(x,t) = c_k^{ads}(x,\tau_{ads}), a_k^{des}(t) = a_k^{ads}(\tau_{ads}),$ $T_g^{des}(x,t) = T_g^{ads}(x,\tau_{ads}),$ (6′) $T_a^{des}(x,t) = T_a^{ads}(x,\tau_{ads}), \quad \nu_g^{des}(x,t) = \nu_g^{ads}(x,\tau_{ads})$
Boundary conditions	
$(n-1)(1+\theta)\tau_{ads} \le t \le (n+n\theta-\theta)\tau_{ads}, n=1,2,...$	$(n+n\theta-\theta)\tau_{ads} < t \le n(1+\theta)\tau_{ads}, n=1,2,...$
$x = 0:$	
$c_k(0,t) = c_k^{in}(t), \quad T_g(0,t) = T_g^{in}(t),$ $\frac{\partial T_a(0,t)}{\partial x} = \alpha S_u(T_a(0,t) - T_g^{in}(t)), \nu_g(0,t) = G^{in}/\varepsilon S$ (7)	$\frac{\partial c_k(0,t)}{\partial x} = 0, \quad \frac{\partial T_g(0,t)}{\partial x} = 0,$ $\frac{\partial T_a(0,t)}{\partial x} = \alpha S_u(T_a(0,t) - T_g(0,t)), \frac{\partial \nu_g(0,t)}{\partial x} = 0$ (7′)
$x = L:$	
$\frac{\partial c_k(L,t)}{\partial x} = 0, \quad \frac{\partial T_g(L,t)}{\partial x} = 0,$ $\frac{\partial T_a(L,t)}{\partial x} = \alpha S_u(T_a(L,t) - T_g(L,t)), \frac{\partial \nu_g(L,t)}{\partial x} = 0.$ (8)	$c_k(L,t) = c_k^{ads}(L,t), \quad T_g(L,t) = T_g^{ads}(L,t),$ $\frac{\partial T_a(L,t)}{\partial x} = \alpha S_u(T_a(L,t) - T_g^{ads}(L,t)),$ $\nu_g(L,t) = G^{out}/\varepsilon S$ (8′)

Table 3

Formulas for calculating the coefficients of the model (1) – (8)

$$D_g^k = 0{,}7 D_{gm}^k + r_{gr} \nu_g \tag{9}$$

$$D_{gm}^1 = (c_2 + c_3)\frac{1}{\dfrac{c_2}{D_{12}} + \dfrac{c_3}{D_{13}}}; \quad D_{gm}^2 = (c_1 + c_3)\frac{1}{\dfrac{c_1}{D_{12}} + \dfrac{c_3}{D_{23}}}; \quad D_{gm}^3 = (c_1 + c_2)\frac{1}{\dfrac{c_1}{D_{13}} + \dfrac{c_2}{D_{23}}}; \tag{10}$$

$$D_{12} = \frac{10^{-7} T_g^{\,1{,}75}\left[\dfrac{(M_{g1}+M_{g2})}{M_{g1}M_{g2}}\right]^{\frac{1}{2}}}{P\left(\vartheta_1^{\frac{1}{3}} + \vartheta_2^{\frac{1}{3}}\right)^2}; \quad D_{23} = \frac{10^{-7} T_g^{\,1{,}75}\left[\dfrac{(M_{g2}+M_{g3})}{M_{g2}M_{g3}}\right]^{\frac{1}{2}}}{P\left(\vartheta_2^{\frac{1}{3}} + \vartheta_3^{\frac{1}{3}}\right)^2};$$

$$D_{13} = \frac{10^{-7} T_g^{\,1{,}75}\left[\dfrac{(M_{g1}+M_{g3})}{M_{g1}M_{g3}}\right]^{\frac{1}{2}}}{P\left(\vartheta_{g1}^{\frac{1}{3}} + \vartheta_{g3}^{\frac{1}{3}}\right)^2};$$

$$\tag{11}$$

$$\beta_K^{1(0)} = A\,\mathrm{Re}^m\,Sc^n\,\frac{D_{H_K}}{4 r_{gr}^2}4; \quad \mathrm{Re} = \frac{4}{3}\frac{\omega \varepsilon \rho_g \nu_{gr}}{\mu_g(1-\varepsilon)}; \quad Sc = \frac{\mu_g}{\rho_g D_{H_K}}; \tag{12}$$

$$\beta_K^{2(0)} = 15\frac{D_{H_K}\varepsilon}{r_{gr}^2 K^2}; \tag{13}$$

$$\alpha_g = \frac{0{,}12\,\mathrm{Re}^{0{,}83}\lambda_g}{r_{gr}}; \tag{14}$$

$$\lambda_g = \frac{1}{2}\left(\lambda_1 c_1 + \lambda_2 c_2 + \lambda_3 c_3 + \frac{1}{\dfrac{c_1}{\lambda_1} + \dfrac{c_2}{\lambda_2} + \dfrac{c_3}{\lambda_3}}\right) \quad \lambda_k = \lambda_{k,0} + \Delta\lambda_{k,1}(T_g - 273{,}15), \quad k = 1, 2, 3; \tag{15}$$

$$P = \rho_g R T_g,\ \rho_g = \sum_{k=1}^{k=3} c_k; \tag{16}$$

$$a_k^* = \frac{(b_{1,k} - b_{2,k}T_a)b_{3,k}\,\mathrm{e}^{b_{4,k}/T_a}\,c_k^{(b_{5,k}+b_{6,k}/T_a)}}{1 + \sum\limits_{n=1}^{3} b_{3,n}\,\mathrm{e}^{b_{4,n}/T_a}\,c_n^{(b_{5,n}+b_{6,n}/T_a)}}, \quad k = 1, 2, 3; \tag{17}$$

$$\left\{ a_k = \frac{(b_{1,k} - b_{2,k}T_a)b_{3,k}\,\mathrm{e}^{b_{4,k}/T_a}\,c_k^{*\,(b_{5,k}+b_{6,k}/T_a)}}{1 + \sum\limits_{n=1}^{3} b_{3,n}\,\mathrm{e}^{b_{4,n}/T_a}\,c_n^{*\,(b_{5,n}+b_{6,n}/T_a)}}, \quad k = 1, 2, 3; \right. \tag{18}$$

$$c_v^g = 10^{-3}(T_g - 273{,}15)\sum_{k=1}^{n_k} c_k\left(A_k + B_k T_g + C_k T_g^2 + D_k T_g^3\right); \tag{19}$$

$$\mu_g = \frac{\mu_1 c_1}{\sum\limits_{j=1}^{3} c_1\sqrt{\dfrac{M_1}{M_j}}} + \frac{\mu_2 c_2}{\sum\limits_{j=1}^{3} c_2\sqrt{\dfrac{M_2}{M_j}}} + \frac{\mu_3 c_3}{\sum\limits_{j=1}^{3} c_3\sqrt{\dfrac{M_3}{M_j}}}.$$

$$\tag{20}$$

coefficient $\beta_k^{2(0)}$ were calculated using formulas (12), (13) [10], where D_{H_K} are the normal diffusion coefficients H_2, CO_2, CO; A, m, n are approximation coefficients, d_q is the equivalent diameter of the channels between the granules $d_q = \dfrac{4\varepsilon r_{gr}}{3(1-\varepsilon)}$, m;

K is the tortuosity coefficient of the pore channels in the adsorbent [12]. The initial approximation θ was assumed to be equal to 1. The heat transfer coefficient α from the surface of the adsorbent granules to the gas mixture flow was calculated using formula (14) where: λ_g is the thermal conductivity coefficient of the gas mixture calculated by formula (15), where values $\lambda_{k,0}$, $\lambda_{k,1}$ for the corresponding component and the thermal conductivity coefficient of the adsorbent λ_a for zeolite CaA are calculated according to [3]. The current pressure values in the Ergun equation (5) were calculated through the concentrations of the components in the gas phase using formula (16). In calculating the equilibrium values of the concentrations of the components in the solid phase a_k^*, using formula (17), the parameters $b_{1-6,k}$ of adsorption isotherms H_2, CO_2, CO on CaA zeolite were used [8]. The values of the equilibrium concentrations of the components in the gas phase c_k^* were determined from the solution of the system of equations (18). Formula (19) for calculating the specific heat capacity of the gas mixture c_v^g and the approximating polynomial coefficients A_k, B_k, C_k, D_k for gases H_2, CO_2, CO were borrowed from the literature [10]. The coefficient of dynamic viscosity of the gas mixture μ_g was calculated by the Herning–Zipperer method [10].

The volumetric flow rate directed to the receiver P (Fig. 1) was determined as $G^P = G^{out} - G^a$, where $G^a = \chi G^{in} \dfrac{P^d}{P^a}$ is part of the input flow directed to CO_2 and CO desorption and discharge into the atmosphere, χ is the reflux ratio [1].

Thus, equations (1) – (20) reperesent a mathematical description of cyclic adsorption-desorption processes carried out in adsorbers $A_1 - A_4$ (see Fig. 1).

The mathematical description of the adsorption-desorption processes taking place in the adsorber includes a system of differential and algebraic equations. To solve a system of partial differential equations, we will use the method of lines. Let us replace the spatial coordinate derivatives x by finite-difference formulas and seek the solution of the

boundary-value problem (the system of differential equations in ordinary derivatives) by the fourth-order Runge–Kutta method along some family of lines.

The algorithm for solving equations (1) – (5) with the initial and boundary conditions (6) – (8) and design formulas for coefficients (9) – (20) is given in [13].

The mismatch of the design values in each cycle at the adsorption stage is estimated on the basis of the material balance on hydrogen

$$E = \int_0^{\tau_a} \left(v_g(0,t)c_1(0,t) - v_g(L,t)c_1(L,t) \right) dt -$$

$$- \int_0^L \left(c_1(x,\tau_a) - c_1(x,0) + \rho_a \left(\frac{1-\varepsilon_0}{\varepsilon_0} \right)(a_1(x,\tau_a) - a_1(x,0)) \right) dx.$$

The adequacy of the mathematical model was checked by the results of independent experiments, i.e. different from the experimental data used to identify the model.

Further, the concentrations of hydrogen, carbon dioxide and monoxide will be denoted by $y = (y_1, y_2, y_3)$ % vol.

The results of the solution of the problem of parametric identification of the mathematical model of the adsorption hydrogen production in a 4-column PSA unit are shown in Fig. 3.

To evaluate the accuracy of the model, we used a function in the form

$$\delta(t) = \left(\left| y_1^{out,e}(t) - y_1^{out}(t) \right| \middle/ y_1^{out,e}(t) \right) 100 \text{ %}.$$

The maximum relative error $\delta(t)$ of the mismatching between the values calculated by the model y_1^{out} and the experimental data $y_1^{out,e}$ at the adsorption stage does not exceed 11.4 %, which makes it possible to use the model for the purposes of technological calculation, optimization and control of the process of hydrogen production by the method of adsorption separation of a gas mixture with an accuracy acceptable in practice.

The mathematical description of the operation mode of the valves is described by the cyclogram $\mathbf{u} = \mathbf{u}(\tau)$ (not shown in the the Figure) according to Table 1, where $\mathbf{u}$ is a vector-function whose components are Boolean variables taking the values 0 or 1. Gas flow rates through the shut-off valves K1.1 – K4.1; K1.2 – K4.2; K1.3 – K4.3; K12; K13; K14; K23; K24; K34 are determined from the solution of the following system:

$$G_{1.1} = k_V \Delta P_{1.1} u_{1.1}; \; G_{2.1} = k_V \Delta P_{2.1} u_{2.1};$$

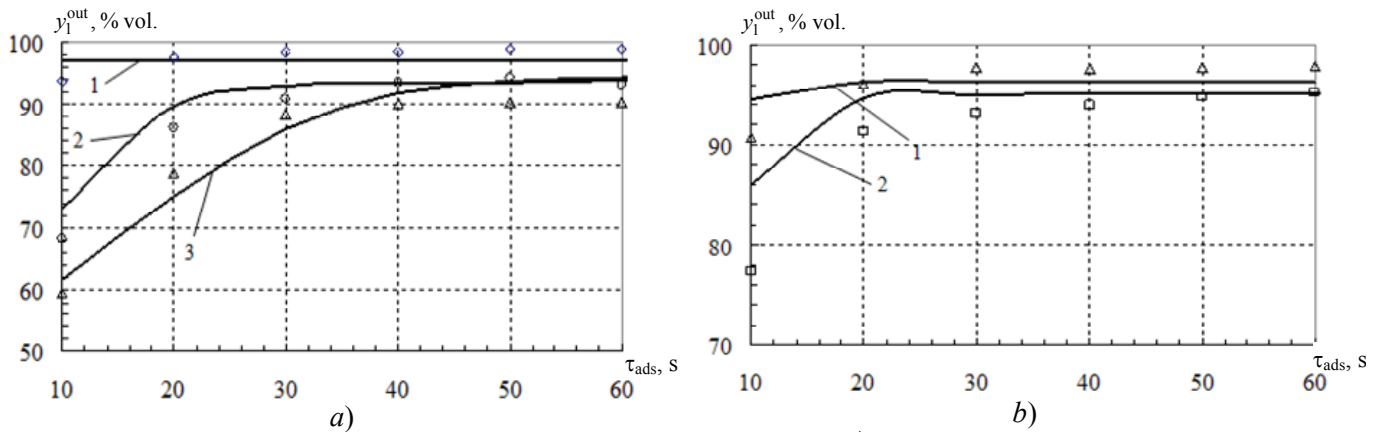$$G_{3.1} = k_V \Delta P_{3.1} u_{3.1}; \; G_{4.1} = k_V \Delta P_{4.1} u_{4.1};$$

Fig. 3. Dynamics of the changes in the hydrogen concentration y_1^{out},% vol. at the output of the PSA unit at the CO₂ concentration in the initial mixture $1 – 10$ % vol.; $2 – 40$ % vol.; $3 – 50$ % vol. (*a*); $1 – 20$ % vol.; $2 – 30$ % vol. (*b*): ◊, ○, △ – experiment, solid line – calculation by the model

$$G_{1.2} = k_V \Delta P_{1.2} u_{1.2} \; ; \; G_{2.2} = k_V \Delta P_{2.2} u_{2.2} \; ;$$
$$G_{3.2} = k_V \Delta P_{3.2} u_{3.2} \; ; \; G_{4.2} = k_V \Delta P_{4.2} u_{4.2} \; ;$$
$$G_{1.3} = k_V \Delta P_{1.3} u_{1.3} \; ; \; G_{2.3} = k_V \Delta P_{2.3} u_{2.3} \; ;$$
$$G_{3.3} = k_V \Delta P_{3.3} u_{3.3} \; ; \; G_{4.3} = k_V \Delta P_{4.3} u_{4.3} \; ;$$
$$G_{12} = k_V \Delta P_{12} u_{12} \; ; \; G_{13} = k_V \Delta P_{13} u13 \; ;$$
$$G_{14} = k_V \Delta P_{14} u_{14} \; ;$$
$$G_{23} = k_V \Delta P_{23} u_{23} \; ; \; G_{24} = k_V \Delta P_{24} u_{24} \; ;$$
$$G_{34} = k_V \Delta P_{34} u_{34} \; .$$

where k_V is the capacity of valves K1.1 – K4.1, K1.2 – K4.2, K1.3 – K4.3, K12, K13, K14, K23, K24, K34; ΔP is a pressure drop on the specified valves; u_{ij} is components of vector **u**, which determine the state variables of the valves.

The flow through the control valve K₅ is calculated by the formula

$$G_5 = k_V^5 \psi_5 \Delta P \; ,$$

where k_V^5 is the capacity of valve K5; ψ_5 is valve opening degree K₅; ΔP is pressure drop on valve K₅.

The mathematical description of the receiver includes the equations of dynamics ofpressure and concentrations of gas mixture components.

The equation of pressure dynamics in the receiver is described by the equation

$$V_m \frac{V_{res}}{RT_g} \frac{dP_{res}}{dt} = G^* - G_p \; ,$$

with initial condition $P_{res}(0) = P^*$; where V_m is molar volume, m³/mol; V_{res} is volume of the receiver, m³;

P_{res} is gas mixture pressure in the receiver, Pa; G_p is flow rate of the consumed production gas mixture, m³/s, G^* is flow rate of the production gas mixture from adsorbers A₁ – A₄, m³/s is defined by the following logical expression

$$G^* = G_{1.2} u_{1.2} \vee G_{2.2} u_{2.2} \vee G_{3.2} u_{3.2} \vee G_{4.2} u_{4.2} .$$

The equation of the dynamics of the changes in the components concentrations ($1 – H_2$; $2 – CO_2$; $3 – CO$) of the gas mixture in the receiver is described by the equation

$$\frac{dc_{k,res}^{out}}{dt} = \frac{1}{V_{res}} \left(G^* c_{k,res}^{in} - G_p c_{k,res}^{out} \right) \; , \; k = 1, 2, 3,$$

with initial condition $c_{k,res}^{out}(0) = c_{k,res}^{out,0}$.

Numerical Investigation of Gas Mixture Enrichment with Hydrogen

Analysis of the PSA process of gas mixture enrichment with hydrogen as an object of research made it possible to determine [13, 14] (Fig. 4): input
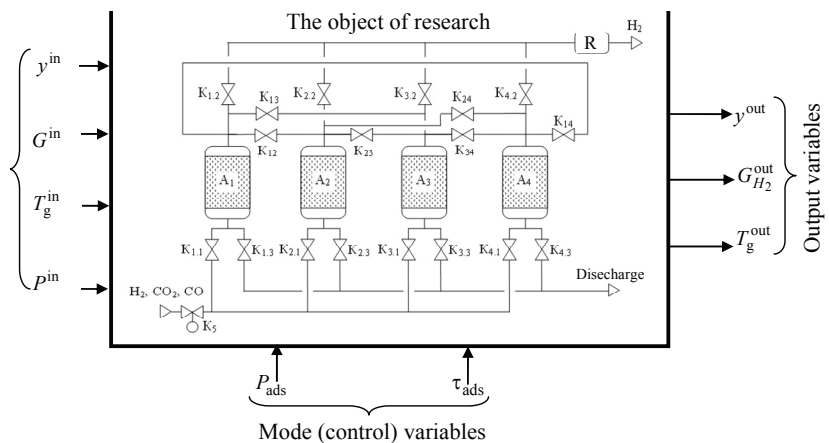

Fig. 4. Scheme of the 4-column PSA unit as an object of investigation in the production of hydrogen:
A₁ – A₄ – adsorbers; K – controlled valves; R – receiver

variables (composition $y^{in} = (y_1^{in}, y_2^{in}, y_3^{in})$, temperature T_g^{in} and pressure P^{in} of the initial gas mixture); mode (control) variables (pressure P_{ads} and cycle duration τ_{ads} of the adsorption stage); output variables (composition $y^{out} = (y_1^{out}, y_2^{out}, y_3^{out})$, flow rate G^{out} and temperature T_g^{out} of the gas mixture at the output of the PSA unit, unit output $G_{H_2}^{out} = y_1^{out} G^{out}$).

Computational experiments were performed to numerically study the effect of input variables and control actions on the output variables of the process of adsorption separation of a gas mixture and hydrogen production. Varying variables and size of their changes are presented in Table 4.

Figure 5 shows the design graphs of pressure changes in adsorbers $A_1 - A_4$ depending on time. The dynamics of the pressure changes in the adsorbers fully corresponds to the cyclogram (Table 1) of the pressure change in the 4-column unit for hydrogen production.

Consider the operation of the unit using adsorber A_1 as an example. The initial rectilinear section in Fig. 5 (segment 1–2) corresponds to the adsorption stage. We note that all the sections with constant pressure correspond to the course of the adsorption process.

At the time moment corresponding to point 2, the adsorption process in adsorber A_1 is completed and the gas, filling it, is discharged into adsorber A_3, at the same time the pressure in A_1 decreases, while the pressure in A_3 increases (segment 2–3). At point 3, the remaining gas from adsorber A_1 is fed to the counterflow purge of adsorber A_4, in so doing, the pressure in A_1 continues to fall (section 3–4). When the adsorbent in the adsorber A_4 is completely restored (point 4), the pressure in A_4 slightly increases, while the pressure in A_1 it continues to fall (segment 4–5).

Table 4

Initial data for a computational experiment

Parameter name	Size of changes
Adsorption stage duration, τ_{ads}, s	$25 - 200$
The ratio of desorption stage duration to adsorption stage duration, $\gamma = \tau_{des} / \tau_{ads}$, rel.units	$0,2 - 0,8$
Carbon dioxide concentration y_2^{in} in the initial mixture (concentration of carbon oxide y_3^{in} remains unchanged and equal to 1 % vol.), % vol.	$25 - 45$
Initial mixture temperature, T_g^{in}, °C	$10 - 50$
Initial gas mixture pressure, P^{in}, MPa	$0,5 - 3$
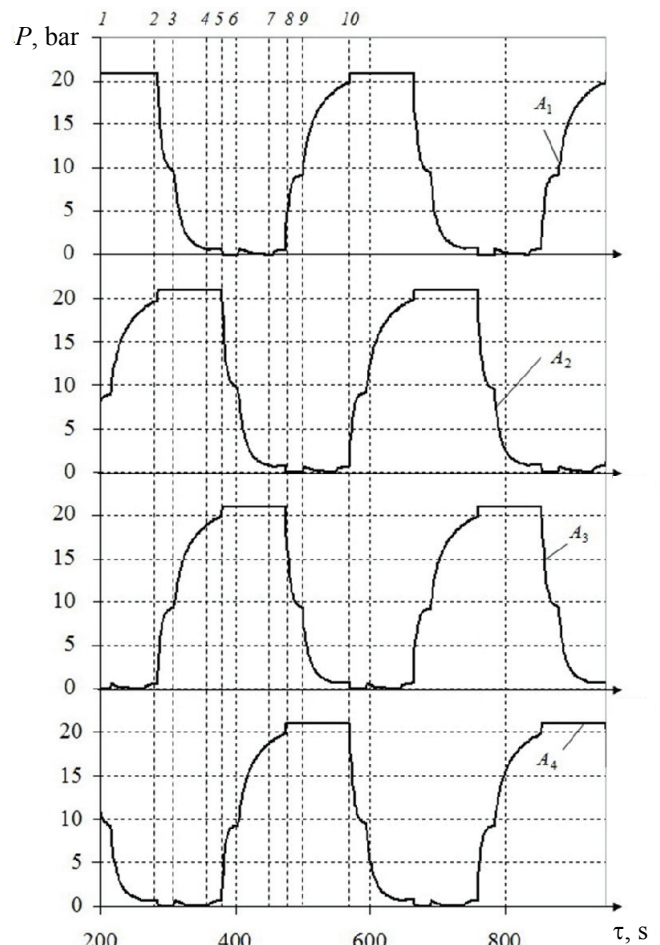
Fig. 5. Pressure dynamics in adsorbers $A_1 - A_4$

At point 5, gas supply from adsorber A_1 to A_4 is stopped, the rest of the gas from A_1 is discharged into the atmosphere, the excess gas pressure in it drops to zero (segment 5–6).

The adsorbent regeneration in A_1 starts at point 6. The production gas from adsorber A_2 is fed with counterflow into adsorber A_1 and reduces the gas pressure therein. The purge ends at point 7, then the pressure in adsorber A_1 begins to increase, and in A_2 it falls (segment 7–8).

In segment 8–9, further pressure rise in A_1 is produced by the gas from adsorber A_3, in which the pressure decreases.

In the last section 9–10, the pressure in adsorber A_1 is brought to the working pressure of adsorption by feeding the initial gas mixture, after which the cycle is repeated.

Similarly, time-shifted cyclic adsorption-desorption processes are carried out in adsorbers A_2, A_3 and A_4.

The analysis of the graphs in Fig. 6, *a* shows that with increasing y_2^{in} the concentration y_1^{out} decreases. So at $y_2^{in} = 34$ % vol. in a time interval $50s \leq \tau_{ads} > 125s$ the concentration of production

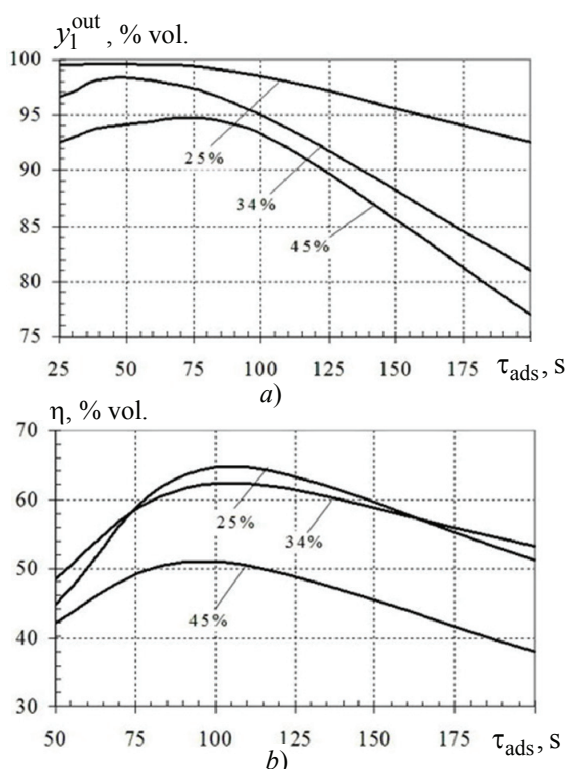Fig. 6. Dependences y_1^{out} and η on τ_{ads} at $\gamma = 0.5$, the temperature of the initial mixture $T_g^{in} = 30 \,°C$ and $y_2^{in} = 25, 34$ and $45\,\%$ vol., respectively

Fig. 7. Dependence y_1^{out} on P^{in} at $\tau_{ads} = 50\,s$ and $\gamma = 0.5$:
$a - y_2^{in} = 34\,\%$ vol., $T_g^{in} = 10, 30, 50\,°C$, respectively;
$b - T_g^{in} = 30\,°C$, $y_2^{in} = 25, 34, 45\,\%$ vol., respectively

hydrogen y_1^{out} decreases from 98 % vol. to 80 % vol. The maximum value $y_2^{out} \approx 99.7\,\%$ vol. is reached at $\tau_{ads} \approx 50\,s$ and $y_2^{in} = 25\,\%$ vol.

As can be seen from the graphs in Fig. 6, *b*, the dependence of the degree of hydrogen extraction η on the duration of the adsorption stage is also of extreme nature. The maximum degree of extraction η according to the graph is reached at $\tau_{ads} \approx 100\,s$ and $y_2^{in} = 25\,\%$ vol. The increase in y_2^{in} concentration leads to η decrease, while the sensitivity of η to a change in y_2^{in} also increases.

From the analysis of the graphs in Fig. 7, *b* it follows that the dependencies are extreme. The maximum purity of the product with CO_2 content $y_2^{in} = 45\,\%$ is observed at $\approx 0.75\,MPa$. With a decrease in the fraction of CO_2 in the initial mixture, the maximum shifts to the right; at $y_2^{in} = 25\,\%$ the graph practically becomes a kind of the saturation curve.

The concentration y_1^{out} of production hydrogen H_2 is inversely proportional to the output at all the considered temperatures and CO_2 concentrations in the initial gas mixture (not shown in the Fig. 7). An increase in the productivity $G_{H_2}^{out}$ of the PSA unit results in the desorption of the adsorbate, being insufficiently produced during the regeneration stage,

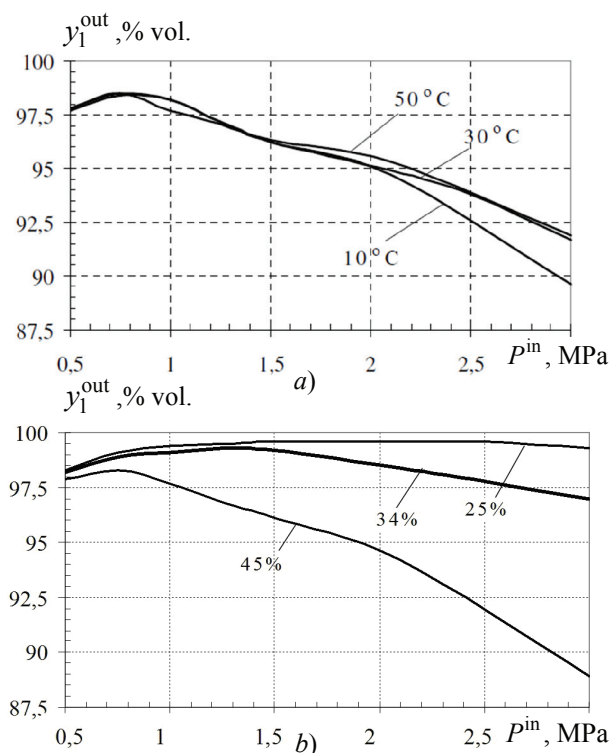which leads to a decrease in the absorption capacity of the adsorbent and the purity of the product obtained. For small values of productivity $G_{H_2}^{out}$, the purity of the product is practically constant and equal to its limiting value for these conditions, the curves tend to saturate, and for values of productivity $G_{H_2}^{out}$ above a certain threshold y_1^{out} they start to decrease noticeably (the dependence is practically linear), and the value of this threshold depends on T_g^{in}. At $T_g^{in} = 50\,°C$ the productivity $G_{H_2}^{out}$ is $550 \cdot 10^{-5}\,m^3/s$, at $T_g^{in} = 10, 30\,°C - 250 \cdot 10^{-5}\,m^3/s$.

The greatest sensitivity y_1^{out} to a change in PSA unit output $G_{H_2}^{out}$ is observed at $y_2^{in} = 45\,\%$ vol., and at $y_2^{in} = 25\,\%$ vol., a decrease in y_1^{out} is insignificant. This means that an increase in T^{in} in some limits or a decrease in y_2^{in} of up to 25 % vol. can significantly improve the unit's output $G_{H_2}^{out}$ with little or no reduction in y_1^{out}.

Temperature T_g^{out} of the production H_2 is proportional to the unit output $G_{H_2}^{out}$ at all the considered values of y_2^{in} (the dependence is not shown in the Figure). The highest value of $T_g^{out} = 323\,K$ is observed at $y_2^{in} = 45\,\%$ vol., which is explained by the high

values of CO_2 concentration in the adsorbent and, as a consequence, by the large thermal effect of the adsorption process. With a decrease in the portion of the impurity in the initial gas, T_g^{out} falls, at $y_2^{in} = 25$ % vol. the lowest sensitivity T_g^{out} to the PSA unit output $G_{H_2}^{out}$ is observed.

Figure 8, *a*, *b* demonstrates the graphs of the change in the sorption value a_2 and CO_2 concentration in the gas phase along the height of the adsorbent bed at the adsorption stage at the temperature of the initial mixture $T_g^{in} = 30$ °C; $y_2^{in} = 34$ % vol.; $\gamma = 0.5$ and the adsorption cycle time $\tau_{ads} = 20, 40, 60, 80, 100$ s, respectively.

At the initial moment of time, intensive absorption of CO and CO_2 impurities occurs in the adsorbent's front bed, and then the mode of parallel transfer of the sorption and thermal fronts along the adsorbent bed starts. As can be seen in the Figures, the sorption front of each component is rather strongly "blurred" along the bed, which is related to the mechanism of adsorption of gas mixture components on the CaA zeolite.

Figure 9, *a*, *b* shows the graphs of temperature variation of the adsorbent T_a and the gas velocity v_g along the height of the adsorbent bed in the adsorption stage for different values of the adsorption cycle time τ_{ads}. During the adsorption, an intensive adsorption of adsorbate (H_2, CO_2, CO) and heat release take place in the front adsorbent bed, which leads to a significant increase in the adsorbent temperature up to 328 – 348 K.
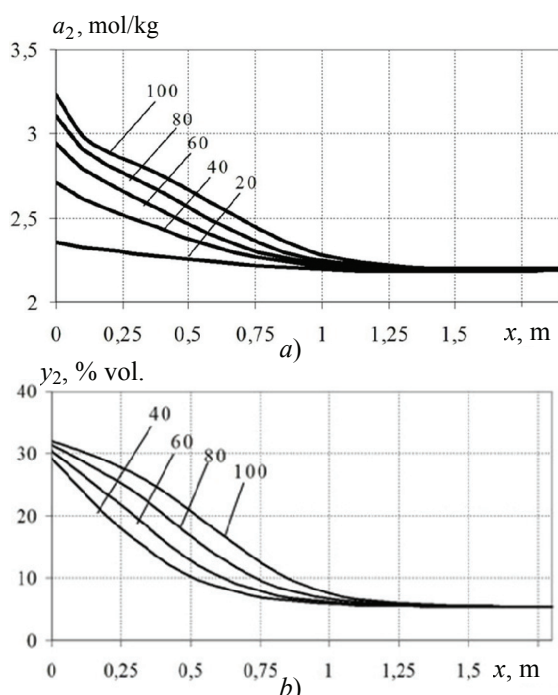

Fig. 8. Change in concentration a_2, y_2 along
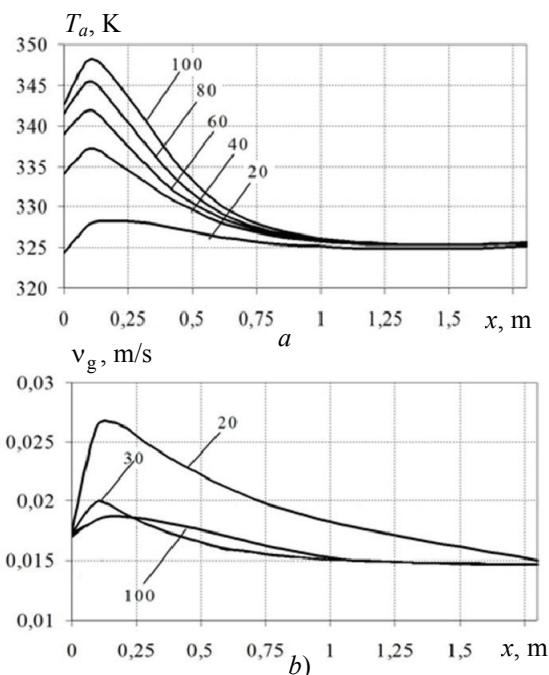the height of the adsorbent bed

**Fig. 9. Variation in the adsorbent temperature
and gas mixture velocity along the height of the bed during the
adsorption stage at values of the adsorption cycle time:**
$a - \tau_{ads} = 20, 40, 60, 80, 100$ s; $b - \tau_{ads} = 20, 30, 100$ s

The temperature curves (Fig. 9, *a*) have maximum at some distance from the start of the adsorbent bed, which is explained by the transfer of sorption heat due to the convective flow in the direction of gas motion. The thermal front for the indicated moments of time moves along with the sorption one (Fig. 8). Thus, the heat losses in this mode of operation are minimal, which facilitates desorption of the adsorbate during the regeneration stage without additional adsorbent heating.

The dependence of gas mixture velocity v_g (Fig. 9, *b*) on the height of the adsorbent bed is of an extreme nature, with the maximum velocity being observed in the adsorbent front bed.

The gas velocity curves in the adsorber correlate with the graphs of change in the concentration of carbon dioxide, as the main impurity, and temperature distribution of the adsorbent over the bed height. The change in the composition and temperature of the gas phase in the adsorber leads to a change in such parameters as the dynamic viscosity, density and molar mass of the gas mixture, which determine the nature of flow hydrodynamics, including the change in the gas velocity.

Conclusion

The developed mathematical model of cyclic process of adsorption separation of a gas mixture and hydrogen production can be used to achieve various

goals: 1) to study the dynamics of adsorption processes under the action of various disturbances (uncertainties in the parameters of raw materials, technological variables) and regions of admissible modes of functioning in the space of control and disturbing actions; 2) to set and solve the problem of optimizing the process of adsorption separation of a gas mixture and obtaining hydrogen of maximum purity; 3) to develop an algorithm and adaptive control system for a cyclic process of adsorption separation of a gas mixture and hydrogen production with an operative change of tasks for regulators of an automatic control system.

On the basis of modern methods of system analysis and mathematical modeling, new scientific results have been obtained for designing automated processes and adsorption process units with cyclically changing pressure for separation of multicomponent gas mixtures.

During the computational experiments it was found that the greatest sensitivity of concentration y_1^{out} and the degree of extraction η of production hydrogen is observed with respect to the duration of the cycle τ_{ads} of the adsorption stage, composition $y^{in} = (y_1^{in}, y_2^{in}, y_3^{in})$, flow rate G^{in}, temperature T_g^{in} and pressure P^{in} of the gas mixture at the PSA unit inlet: 1) the maximum concentration value $y_1^{out} \approx 99.7\ \%$ is achieved at $\tau_{ads} \approx 50$ s, $y_2^{in} = 25\%$ vol. and the temperature of the initial gas mixture $T_g^{in} = 30\ °C$; 2) at $T_g^{in} = 50\ °C$ the unit output $G_{H_2}^{out}$ is $550 \cdot 10^{-5}$ m^3/s, and at $T_g^{in} = 10, 30\ °C - 250 \cdot 10^{-5}$ m^3/s; 3) the adsorbent temperature reaches its maximum value in the front bed (at $\tau_{ads} = 100$ s $- T_a = 348$ K, at $\tau_{ads} = 20$ s $- T_a = 328$ K), and in the depth of the bed T_a decreases to a temperature $T_a = 325$ K for all τ_{ads} values.

Numerical studies of the process of hydrogen production by PSA method of the separation of a multicomponent gas mixture made it possible to determine the most dangerous disturbances (composition $y^{in} = (y_1^{in}, y_2^{in}, y_3^{in})$, temperature T_g^{in} and pressure P^{in} of the gas mixture at the inlet of the PSA unit) and efficient control (gas mixture flow rate G^{in}, adsorption stage cycle duration τ_{ads}) actions needed for setting a problem of dynamic optimization and control of the process of adsorption hydrogen production.

Acknowledgement

References

1. Shumyatskiy Yu.I. *Promyishlennyie adsorbtsionnyie protsessyi* [*Industrial adsorption processes*]. M.: KolosS, 2009. 183 p. (Rus)

2. Ruthven D.M., Farooq S., Knaebel K.S. *Pressure swing adsorption*. New York, 1993.

3. Keltsev N.V. *Osnovyi adsorbtsionnoy tehniki* [*Basics of adsorption technique*]. M.: Himiya, 1976. 512 p. (Rus)

4. Mohamed Safdar Allie Baksh, Mark William Ackley. US Patent 6340382. *Pressure swing adsorption process for the production of hydrogen*, 2002.

5. Akulinin E.I., Gladyishev N.F., Dvoretskiy S.I. Perspektivnyie tehnologii i metodyi sozdaniya kompozitsionnyih sorbtsionno aktivnyih materialov dlya tsiklicheskih adsorbtsionnyih protsessov [Perspective technologies and methods for creating composite sorption active materials for cyclic adsorption processes]. *TSTU Transactions*, 2017, vol. 23, no. 1, pp. 85-103. (Rus)

6. Kirillin V.A., Syichev V.V., Sheyndlin A.E. *Tehnicheskaya termodinamika* [*Technical Thermodynamics*]. M.: Izd. dom MEI, 2008. 496 p. (Rus)

7. Akulov A.K. *Modelirovanie razdeleniya binarnyih gazovyih smesey metodom adsorbtsii s koleblyuschimsya davleniem* : dis. ... d-ra tehn. nauk 05.17.08 [*Simulation of the separation of binary gas mixtures by adsorption with an oscillating pressure*]. SPb.: STU, 1996. 304 p. (Rus)

8. Jeong-Geun Jee, Min-Bae Kim, Chang-Ha Lee. Adsorption characteristics of hydrogen mixtures in a layered bed: binary, ternary, and five-component mixtures. *Ind. Eng. Chem. Res.*, 2001, vol. 40, pp. 868-878.

9. Beloglazov I.N. *Osnovyi rascheta filtratsionnyih protsessov* [*Basics of the calculation of filtration processes*]. M.: 2002. 210 p. (Rus)

10. Rid R., Praustnits Dzh., Shervud T. *Svoystva gazov i zhidkostey* [*Properties of gases and liquids*]. L.: Himiya, 1982. (Rus)

11. Galperin N.I. *Osnovnyie protsessyi i apparatyi himicheskoy tehnologii* [*Basic processes and apparatuses of chemical technology*]. M.: Himiya, 1981. 812 p. (Rus)

12. Aerov M.E., Todes O.M. *Gidravlicheskie i teplovyie osnovyi rabotyi apparatov so statsionarnyim i kipyaschim zernistyim sloem* [*Hydraulic and thermal foundations for the operation of devices with a stationary and boiling granular layer*]. L.: Himiya, 1968. 512 p. (Rus)

13. Ishin A.A. *Matematicheskoe modelirovanie i upravlenie protsessom polucheniya vodoroda metodom adsorbtsionnogo razdeleniya gazovoy smesi*: dis. ... kan. tehn. nauk: 05.13.06 [*Mathematical modeling and control of the process of hydrogen production by the method of adsorption separation of a gas mixture*]. Tambov: TSTU, 2017. 152 p. (Rus)

14. Vasilev A.S., Ishin A.A., Skvortsov S.A. Matematicheskoe modelirovanie i optimalnoe upravlenie adsorbtsionnyim protsessom razdeleniya gazovoy smesi [Mathematical modeling and optimal control of the adsorption process of gas mixture separation], *Sistemyi upravleniya i informatsionnyie tehnologii* [*Control Systems and Information Technology*], 2016, no. 4(66), pp. 47-52. (Rus)